https://doi.org/10.5194/os-2021-52
Preprint. Discussion started: 11 June 2021

Ocean Science Discussions
Open Access

Marine Heatwaves in the Arabian Sea

Abhisek Chatterjee[1], Gouri Anil[2], Lakshmi R. Shenoy[1,3]

[1]Indian National Centre for Ocean Information Services, Ministry of Earth Sciences, Hyderabad, India
[2]Cochin University of Science and Technology, Cochin, India
[3]Kerala University of Fisheries and Ocean Studies, Cochin, India
Correspondence to: Abhisek Chatterjee (abhisek.c@incois.gov.in)

Abstract. Marine heatwaves (MHWs) are prolonged warm sea condition events that cause a destructive impact on marine ecosystems. The documentation of MHWs and assessment of their impacts are largely confined to a few regional seas or in global mean studies. The Indian Ocean received almost no attention in this regard despite the fact that this ocean basin, particularly the Arabian Sea, is warming at the most rapid pace among the other tropical basins in recent decades. This study shows the characteristics MHWs for the Arabian Sea during 1982-2019. Our analysis shows that the duration of MHWs exhibit a rapidly increasing trend of ~20 days/decade (1.5-2 count/decade) in the northern Arabian Sea and in the southeastern Arabian Sea close to the west coast of India; which is more than 15 fold increase in the MHW days from the early 80s'. At the same time increase in MHW frequency is ~1.5-2 count/decade i.e an increase of ~ 6 fold, indicating more frequent and much longer heatwave events in the recent decade. Notably, since the beginning of the satellite record, the year 2010 and 2016 saw the maximum number of heatwave days with more than 75% of days of the pre-monsoon and summer monsoon season experienced heatwaves. The accelerated trend of the heatwave days is found to be driven by the rapid rise of the mean SST of the Arabian Sea in the recent decade. Moreover, longer heatwave days are also associated with the dominant climate modes and among them, Indian Ocean Basin mode via the decaying phase of the El-Niño is found to be the most influencing mode contributing in more than 70-80% of observed heatwave days in this basin. Mixed layer heat budget analysis suggests significant heterogeneity in the dominant processes across the years; however, weakening of latent heat loss is in general one of the key mechanism in the genesis of most of the MHWs.

1 Introduction

Sea surface temperature (SST) shows significant variability over a large spectrum of frequencies in space and time across the globe. However, there are times when extremes of such variability occur causing severe stress to the local ecosystem and economies driven by such ecosystems. These warmer than normal extreme ocean conditions are referred to as Marine Heatwaves (MHWs) and are defined as prolonged anomalously warm ocean condition exceeding a pre-defined threshold (Pearce et al., 2011; Hobday et al., 2016). These extreme warm events are shown to be responsible for widespread coral bleaching (Hughes et al., 2017), loss of Kelp forest off the coast of Australia and New Zealand (Wernberg et al., 2016;

https://doi.org/10.5194/os-2021-52
Preprint. Discussion started: 11 June 2021

Thomsen et al., 2019), reduction in seagrass meadows (Arias et al., 2018) and widespread harmful algal blooms (Trainer et al., 2020). Further, these events have also shown to impact economically important fishery industries in the northwest Atlantic (Mills et al., 2013), northeast Pacific (Cavole et al., 2016) and coastal Australia (Caputi et al., 2016). Owing to their devastating nature, MHWs and it's generating mechanisms received a lot of attention in the recent decade. Studies of major MHWs that appeared in various parts of the world over the last decade suggest that evolution and the forcing mechanisms of such events vary considerably from region to region and predominantly depend on the local air-sea coupling, atmospheric conditions, oceanic preconditions and remote climatic teleconnections (Holbrook et al., 2019; Oliver et al., 2021). For example, persistent large scale positive atmospheric pressure anomaly ridge caused unprecedented warm SST in the northeastern Pacific during 2013-2016 with anomalies exceeding more than 3^{o}C (Bond et al., 2015; Lorenzo and Mantua, 2016). A similar mechanism was at play during the summer of 2003 in the Mediterranean Sea (Olita et al., 2006) and in the Tasman Sea during the summer of 2017/18 off the coast of New Zeeland (Salinger et al., 2019). On the other hand, advection of warm water found to be responsible for the widespread MHW in the tropical ocean around Australia in 2015/2016 (Benthuysen et al., 2018), southeast of Australia in the Tasman Sea during 2015/16 (Oliver et al.,2017) and off the coast of California (Durazo et al., 2002). Climate variabilities also play a significant role in modulating MHWs in the tropical/extratropical oceans (Holbrook et al., 2019). Among them El-Niño Southern Oscillation (ENSO) shown to be the dominant climate mode that influences MHW occurrence and duration in the tropical Pacific (Holbrook et al., 2020). In the Indian Ocean, the positive phase of ENSO (Roxy et al., 2014; Chakravorty et al., 2014), Indian Ocean Basin Mode (Klein et al., 1999; Du et al., 2009) and Indian Ocean Dipole mode (Saji et al., 1999; Chowdary and Gnanaseelan, 2007) favour warming of SST in large part of the basin. In the extratropics, MHWs in the northeast Pacific is primarily associated with the positive phase of Pacific Decadal Oscillation (PDO) in interannual time scale and Pacific Decadal Oscillation and North Pacific Gyre Oscillation (NGPO) in longer time scale (Lorenzo and Mantua, 2016). Whereas, North Atlantic oscillation (NAO) shows strong associations in the MHWs of the northwest Atlantic (Scannell et al., 2016).

Unfortunately, while the understanding of the genesis of MHWs across the globe advanced rapidly over the last decade, there is no study even to document these events in the northern Indian Ocean. Moreover, over the last few decades Indian Ocean, particularly the Arabian Sea, sees rapid warming at a rate much faster than the other tropical basins (Levitus et al., 2012). This warming not only show a negative influence on the primary productivity of the Arabian Sea (Roxy et al., 2016) but also influences a shift in the phytoplankton community from diatoms to *Noctuluca scintillans* in the northern Arabian Sea (Goes et al., 2020), reduced rainfall in the Indian continent (Roxy et al., 2015) and increase flood in the Indian mainland (Ajaymohon and Suryachandra, 2008). Moreover, the frequency of cyclogenesis in the Arabian Sea has also increased over the last few decades largely believed to be driven by this rapid rise in the SST. However, the impact of persistent MHW on this enhanced cyclogenesis is still yet to be explored. Further, the southeastern Arabian Sea and the northern Arabian Sea are also economically very important as they constitute one of the major fishing zones in the Arabian Sea. As per the recent report from Central Marine Fisheries Research Institute, India (CMFRI, 2007) total fish landing from the Indian exclusive

https://doi.org/10.5194/os-2021-52
Preprint. Discussion started: 11 June 2021

economic zones (EEZ) is 2.49 × 10^6 tonnes during 2001-2005 and among them, 67% of the catch is from the eastern Arabian Sea (Shankar et al., 2018). Hence, like other parts of the global ocean, MHWs in this region is very likely significantly influencing the local marine ecosystem, the migration of species and the associated fishery-dependent economy. Therefore, documenting and understanding the genesis of MHWs in the Arabian Sea, particularly in the coastal oceans which possess significant economic importance, is necessary for better prediction of these MHWs and assessment of their impacts on this region. Hence, in this study, we document MHWs in the Arabian Sea with a special emphasis on the coastal waters close to the west coast of India and try to decipher the possible physical mechanisms that influence the genesis of such heatwaves in this region. Next, in Section 2 we describe the data we use and the model configuration, experiments and forcing. Section 3 describe the observed trend in the MHWs. The influence of SST trend and the variabilities are given in Section 4. In Section 5, the impact of various climate modes are discussed. In Section 7, the role of various physical processes during some of the strongest heatwaves are presented based on a mixed layer heat budget study and finally, Section 7 summarizes our main results and discuss possible implications of this study.

2 Data and Methodology

2.1 Sea Surface Temperature and MHW Detection

To detect MHWs for the Arabian Sea, we have used daily NOAA OISST version 2 (Reynolds et al., 2007). The SST data are analysed for the period of 1982-2019 available on a 0.25^o × 0.25^o grid. The MHW detection tool "*heatwaveR"* package (Schlegel and Smit, 2018) is used for MHW detection. This tool uses MHW definition based on Hobday et al. (2016) and characterizes MHW as an anomalous, warm, discrete event prolonged for more than 5 continuous days with SST more than a particular threshold. The threshold is defined from a fixed seasonal climatological baseline with warmer SST above the 90th percentile of the daily variability. Two consecutive events within 3 days are considered as a single event. The climatological baseline is defined based on a fixed 30 year period 1982-2011. This seasonally varying threshold allows heatwaves events to occur at any season across the year. In order to understand the MHW characteristics, three heatwave metrics are evaluated here: MHW duration defined as the days between the start and end dates of an event, MHW intensity which refers to maximum SST anomaly during an event and MHW frequency calculated based on the number of events occur during a season or year.

2.2 Ocean Model

The model used in the present study is an ocean general circulation model based on Modular Ocean Model version 5 (MOM5; Griffies, 2012). The model configuration uses a hydrostatic and Boussinesq approximation with model coordinates are discretized based on generalised orthogonal coordinates in horizontal and z*-coordinate in the vertical. The model domain extends from 30^{o}E-120^{o}E and 30^{o}S-30^{o}N with a uniform horizontal resolution of 0.25^o×0.25^o and 40 z* levels in the vertical. The model bathymetry is based on Sindhu et al. (2007) with a minimum depth set to 15 m. The horizontal mixing is based on Griffies & Hallberg, (2000) and the vertical mixing scheme is based on Large et al. (1994). To keep the model stable, the horizontal friction is set to the lowest value. The temperature and salinity fields are relaxed to climatological values (chatterjee et al., 2012) with a time scale of 30 days within the 4^{o} sponge layer at the open eastern and southern boundaries. Salinity at the surface is restored with a relaxation of 15 days. To realistically simulate the cross basin flow, the narrow Palk strait between India and Sri Lanka is closed in this model (Chatterjee et al., 2013, 2017).

2.2.1 Model experiments and forcing

The model is initially spin-up for 35 years from a state of rest and then the interannual run was carried out for 1990-2018 using restart state of the ocean from the final year simulation of the climatological run. For forcing the model, surface momentum fluxes (zonal and meridional wind stress) and surface heat fluxes (shortwave radiation, longwave radiation, air temperature and 2 m specific humidity) are obtained from Tropflux data (Praveen et al., 2012, 2013). The precipitation and surface air pressure are obtained from NCEP reanalysis product (Kalnay et al., 1996). The monthly climatological river discharge is based on Vörösmarty et al. (1996) and Papa et al. (2010) and is introduced over the top 15 m of the water column. The model is extensively validated for the north Indian Ocean in earlier studies (Chatterjee et al., 2013, 2019; Shankar et al., 2016, 2018; Vijith et al., 2016; Lakshmi et al., 2020). In order to analyse model simulated anomaly for each variables, this 29 years interannual simulation is used to calculate a climatological field.

2.2.2 Mixed layer heat budget

In order to understand the dominant physical forcing in the genesis of MHWs a volume-averaged mixed layer heat budget analysis has been carried out using the temperature and velocity fields taken from the model simulation. The mixed layer temperature tendency over the time-varying mixed layer and fixed region of area A is given by

$$\frac{\partial \overline{T}}{\partial t} = \underbrace{-\overline{\nabla_H T}}_{Adv_H} + \underbrace{\frac{1}{\rho C_P}\int_A \frac{Q}{h} dA}_{Q_v} \underbrace{-\overline{w\frac{\partial T}{\partial z}} - \frac{1}{Ah}\int_A \left(k_v \frac{\partial T}{\partial z}\right)_{-h}}_{Subsurface\ Process} \quad (1)$$

Where T is the SST, t is time, overbar represents volume averaged over the region A and within the time-varying mixed layer depth h. Adv_H is the horizontal advection of temperature, Q is the net surface heat flux corrected for shortwave penetration below the surface mixed layer, ρC_P is the specific heat capacity of seawater, w represents the vertical velocity and k_v is the vertical eddy diffusivity. The vertical advection and diffusion together represent subsurface processes that influence mixed layer temperature.

https://doi.org/10.5194/os-2021-52
Preprint. Discussion started: 11 June 2021

3 Trends in the MHW

Figure 1 shows the trend of various MHWs characteristics of the Arabian Sea (north of 5^{o}N). The number of MHW days increased significantly over the entire Arabian Sea (Figure 1a). The northern Arabian Sea and the southern Arabian Sea show the strongest annual increasing trend with a rate of ~3 days/year. A similar increasing trend is also noticeable in the Persian Gulf and the Gulf of Aden, two marginal seas connected to the Arabian Sea. The rest of the Arabian Sea, including the coastal water of India, shows an annual increase in the MHW days at a rate of 1.5-2 days/year. Note that the north Indian ocean sees rapid warming during the pre-monsoon or spring intermonsoon (PRM; March-April-May) and the summer monsoon (SWM; June-July-August-September) seasons when the Inter-Tropical Convergence Zone moves to the northern hemisphere over the Indian landmasses. This is the time, the Indian Ocean warm pool covers a large part of the southern and eastern part of the Arabian Sea and the SST reaches more close to 31^{o}C (Joseph, 1990; Vinayachandran and Shetye, 1991; Shenoi et al., 1999; Chatterjee et al., 2012). Therefore, it is likely that this mean SST rise during these two seasons possibly has a large impact on the MHW genesis over this region. Hence, the characteristics of these extreme events during the PRM and SWM seasons are investigated separately. Interestingly, PRM and SWM constitute most of the marine heatwave days observed annually across the years with about 60% of heatwaves days occur during these two seasons in the Arabain Sea. Moreover, the trends of the heatwave days show marked spatial contrast between the two seasons (Figure 1d, g). During PRM season, the strongest trend is primarily limited to the northern Arabain Sea along the coast of Pakistan, the northwestern coast of India (coast of Gujarat and Maharastra) and in the western boundary of the Arabian Sea along the coast of Arabia and Somalia. Whereas, the rest of the Arabian Sea does not show any notable increase in heatwave days. On the other hand, during SWM, a significant increase in heatwave days is observed in the southeastern Arabian Sea, particularly all along the west coast of India. Additionally, the northern Arabian Sea continues to show a significant increasing trend similar to the PRM season but now limited mostly along the coast of Pakistan. During this season the western Arabian Sea does not show any significant trend in heatwave days.

The frequency of heatwaves also show a marginal annual increasing trend across the Arabian Sea, but the stronger trend of ~0.06-0.08 count/year is limited to the southern and northeastern Arabian Sea and all along the west coast of India (Figure 1b). During PRM and SWM season, the increasing trend of heatwave frequency is mostly collocated with the regions where an increasing trend of heatwave days is observed (Figure 1e, h). Therefore, while during PRM season an increasing trend in frequency is observed in the northern Arabian Sea region at a rate of ~0.1–0.15 count/year, the SWM season shows a similar trend along the west coast of India and across the southeastern Arabian Sea region. Note here that, annually while the increase in the number of heatwaves over the four decades is only about 3-4 counts, the heatwave days have increased by about 80-120 days. This means that the increase in heatwave events is much smaller compared to the observed increase in heatwave days annually; indicating that in the recent decades the heatwaves have turned much prolonged than that of the early 80s' and 90s'. On the other hand, heatwave intensity shows a meagre increase over most part of the Arabian Sea. The

https://doi.org/10.5194/os-2021-52
Preprint. Discussion started: 11 June 2021

most intense MHW intensity is experienced in northern Arabian Sea where an increasing rate of ~0.05°C/year is observed during the PRM season.

Next, in order to understand the heatwave mechanisms in detail, based on the observed trend of the various heatwave characteristics, we have selected two regions in the Arabian Sea for further analysis: the northern Arabian Sea (NAS; 60°E-70°E,18°N-25°N) and the southeastern Arabian Sea (SEAS ; 65°E-74°E,7°N-16°N) (black boxes in Figure 1). Figure 2 shows the time series of percentage of heatwave days across each year annually and seasons-wise since 1982 for these two selected regions. In both the regions, the number of heatwave days were comparatively low until the year 2000 except for the year 1986/87, 1992 and 1998 coinciding with the decaying phase of the El-Niño and the positive phase of the Indian Ocean Basin Mode (Figure 2a, b). During this pre-2000 era annually only ~5-10% of days experience heatwaves in these regions. Post-2000, the number of heatwave days increase significantly with an average of ~10-20% days experience heatwave in almost all years. Further, the rapid increase in heatwave days is observed from the year 2015 with at least 25-50% of days experience heatwave. During PRM season, the percentage of heatwave days is marginally higher in the NAS compared to the SEAS (Figure 3c, d). Moreover, as noted for annual, during PRM season, NAS shows a marked rise in heatwave days from the year 2015 with consistently more than 25-50% of days experience heatwave in this region. Nevertheless, during the entire satellite era, the year 2010 and 2016 stands out as both regions experience heatwave for almost all days during this season. During SWM season, the characteristics of heatwave days remain similar as was observed in PRM. The only exception is that since 2015, SEAS experiences more heatwave days than the NAS. Particularly, the summer of 2015, 2017 and 2019 sees at least 50% or more heatwave days in the SEAS.

Overall, there is a notable increasing trend of the heatwave days annually and for the PRM and SWM seasons. Interestingly, the rapid increase in MHW days in the last decade coincide with the period of rapid mean SST warming of this region. This indicates that the anthropogenic warming of the mean SST is likely behind this increased heatwaves over this region. Further, most of the intense heatwave years also coincide with the El-Niño year or the year next to the El-Niño year suggesting an important role of climate modes in modulating these extreme events in this region which is in agreement with what is observed in other regional seas across the world ocean.

4 Role of Indian Ocean Warming and SST Variability

The Indian Ocean is warming rapidly over the last few decades. An estimate based on Enhanced Reconstructed Sea Surface Temperature (ERSSTv4) indicates that the tropical Indian Ocean is warming at a rate of 0.15°C/decade during 1951-2015 (Roxy et al., 2020). Notably, during the summer monsoon, the western Arabian Sea experienced anomalous warming of more than ~1.2°C during 1950-2012 (Roxy et al., 2014). SST trend calculated during this study period (1982-2019) for the Arabian Sea indicates that annual anomalous warming of ~1.5°C in the recent decade is limited in the northern part of the

https://doi.org/10.5194/os-2021-52
Preprint. Discussion started: 11 June 2021

Arabian Sea and ~0.75°C in some part of the southern Arabian Sea (Figure 3a). However, the season-wise SST trend shows pronounced spatial contrast between PRM and SWM seasons: while during PRM, NAS experiences anomalous warming of more than ~1.5°C (Figure 3b), during SWM the warming of ~0.75-1°C is located close to the west coast of India (Figure 3c). Interestingly, regions of the this strongest warming trend also experience an increasing trend of MHWs (see Figure 1), indicating that the warming of the mean SST contributes to the increasing trend of heatwave days in the Arabian Sea. This is in agreement with Oliver et al. (2019) who suggest that during the satellite period about 2/3rd of the global ocean experiences an increasing trend of heatwave days due to the rising mean temperature of the ocean.

In order to understand the importance of the mean SST trend and the variability in the SST on the heatwave days over the Arabian Sea, the SST time series is decomposed as below:

$$T(t) = T^{tr}(t) + T^{var}(t), \qquad (2)$$

here, $T(t)$ is the time series of SST, $T^{tr}(t)$ is the SST trend, and $T^{var}(t)$ is the SST anomaly after removing the trend. Figure 4 shows the time series of the percentage of heatwave days based on detrended SST time series (T^{var}). In this case, the duration of MHWs for each year and seasons is primarily due to the variability of SST. The major contrast between heatwave days based on $T(t)$ and $T^{var}(t)$ (Compare Figure 2 and 4) is that there is no secular trend in the heatwave days when calculated based on the only SST variability. This supports that the increasing trend in the MHW days in the Arabian Sea is driven by the rising temperature of the mean SST and not the variability. Noticeably, it is evident that these extreme warm events are a regular phenomenon and existed since the record of satellite observation. Owing to the definition of MHWs, these extreme events in the ’80s and ’90s are underestimated. Note also that SST variability contributed most strongly during the PRM season of 2010 in the NAS region with almost 50-75% of days of this season experienced heatwaves due to SST variability (Figure 4c). The 2016 event was the second most event in this region contributed strongly by the SST variability. In fact, as will see in the next section, we find that these large number of heatwave days during PRM season is primarily driven by El-Niño via the positive phase of Indian Ocean Basin mode. In contrast, in the SEAS, the SST variability contributed most for the year 2016 with almost 20-40% of the observed heatwave days. The other notable years are 1988, 1998 and 2003 when a considerable number of days experience heatwave in this region due to SST variability alone. On the other hand, during the SWM season, the contribution of SST variability is most notable for the year 1982, 1983, 1987, 1988, and 2010 in the NAS and the year 1983, 1987, 2003 and 2015 in the SEAS.

In order to compare the role of mean SST warming with the SST variability, Figure 5 shows that the time series of the ratio of the heatwave days owing to the SST trend and its variability by rearranging Equation (2) as follows:

$$\frac{MHW(T^{tr})}{MHW(T^{var})} = MHW\left(\frac{T}{T^{var}} - 1\right) \approx \frac{MHW(T)}{MHW(T^{var})} - 1 \qquad (3)$$

assuming that MHW based on T^{tr} and T^{var} are independent of each other. This is a fairly good approximation as the seasonal climatology is prepared using a 30 year record and doesn’t include the last decade when rapid increase in SST is

https://doi.org/10.5194/os-2021-52
Preprint. Discussion started: 11 June 2021

observed and thus, can provide usful insight of the role of mean warming trend of the SST on the MHW generation. It shows a very secular shift after the year 2000 in the driving force of the total annual heatwave days in the Arabian Sea. While, during the pre-2000 era the natural variability of SST contributes most in driving the MHWs, post-2000 the warming trend of mean SST becomes the dominant factor. It also shows that the influence of mean SST warming increased very rapidly over the last two decades which is expected to continue further under the unabated Indian Ocean warming. However, there are years when the ratio is much smaller when the climate mode driven variability contributes significantly to these extreme warm events as noted in Figure 4.

5 Role of Dominant Climate Modes

Indian Ocean dipole mode (IOD) and El-Niño Southern Oscillation (ENSO) are the two dominant climate modes that contribute to the SST variability of the tropical Indian Ocean in interannual timescale (Saji et al., 1999; Du et al., 2009). During the positive phase of the IOD, the western Indian Ocean shows anomalous warming, whereas the eastern Indian Ocean cools. In the negative phase, the sign of the SST anomaly reverses. Similarly, ENSO modulates the SST in the tropical Pacific, but the influence of ENSO can be felt in other basins as well through an atmospheric teleconnection via anomalous Walker circulation (Du et al., 2009) and the inter-basin transport of water mass properties (Lee et al., 2015). During the positive phase of ENSO i.e. during El-Niño, the western Indian Ocean shows warmer anomaly due to the weakening of the summer monsoon winds and increased shortwave radiation (Swapna et al., 2014). On the other hand, during La-Nina, most parts of the Indian Ocean experiences cooler anomaly except the west coast of Australia where SST elevated due to heat transport via Leeuwin current (Benthuysen et al., 2014). Associated with the direct impact of ENSO, the Indian Ocean warming mode (also referred to as Indian Ocean Basin mode; IOBM) which peaks during the decaying phase of the El-Niño and after the La-Nina, also contributes to the widespread warming of the tropical Indian Ocean (Xie et al., 2009). Moreover, North Atlantic Oscillation (NAO) also shown to play an important role in modulating SST of the Indian ocean in interannual to decadal time scale (Xie et al., 2021). Therefore, these climate modes can support the genesis or suppression of heatwaves depending upon their phases via modulating the thermocline depth and associated air-sea interactions of the basin (Hobrook et al., 2019, 2020; Oliver et al., 2021).

In this section, we will look at the role of these climate modes, particularly IOD, ENSO, IOBM and NAO on the genesis of MHWs in the Arabian Sea. As noted already in the previous section that the most number of heatwave days observed either during the El-Niño years or during the decaying phase of the El-Niño i.e. during the positive phase of the IOBM. This indicates that the El-Niño and IOBM climate modes play a significant role in modulating heatwaves in this region. Figure 6a shows the correlation between MHW days derived from the detrended SST observation and the above-mentioned climate modes. ENSO shows the strongest correlation in the southcentral Arabian Sea with a correlation coefficient of ~0.5. The correlation decreases northward and in fact, turns negative in the Persian Gulf region. The influence of IOD is most prominent in the western Arabian Sea in the vicinity of the western box of the IOD. Otherwise, the correlation is generally weak for the rest of the basin except close to the coast of Iran and Pakistan where a marginal increase in correlation is observed. However, note here that, unlike ENSO, the spatial and temporal lengthscale of IOD is much smaller and thus, the correlation across the entire year may be less, but can still influence significantly over a larger region during its peak phase. As expected, the IOBM, which represents the basin-wide warming mode of the tropical Indian Ocean, shows the strongest influence on the MHW days with a correlation coefficient of ~0.5 in most part of the Arabian Sea. In this case also, like ENSO, the correlation decreases in the north. The influence of NAO is the weakest among the other climate modes and mostly limited to the SEAS region close to the southern part of the west coast of India during the the negative phase.

As evident in the correlation map, the strong association of IOBM with the MHW days also reflected in the large percentage of heatwaves days that co-occur with the positive phase of the IOBM (Figure 6b). Annually, about 60% and 75% of heatwave days co-occur with the positive IOBM in the NAS and SEAS, respectively. These co-existing numbers go much higher during the PRM season with more than 82% of heatwave days coincide with the positive IOBM phase in the SEAS region. The next most influencing climate mode is the positive phase of ENSO or El-Niño. This is more conspicuous during the PRM season as both the region experiences close to 50% co-existence between heatwave days and El-Niño. On the other hand, positive IOD also significantly co-exist with more than 40% of heatwave days during this season. During the SWM season, this association between IOBM and heatwaves decrease a bit with about 43% and 68% of heatwave days co-occur with the positive IOBM in the NAS and SEAS, respectively. The influence of El-Niño, on the other hand, show marked difference between NAS and SEAS region. During summer, while in the SEAS El-Niño co-occur with ~50% heatwave days; in the NAS, both the phase (i.e. El-Niño and La-Nina) co-occur in ~20% heatwave days. This equal co-occurance of heatwave days in NAS indicates that there is no causal relationship between heatwave and ENSO in this region and therefore, possibly a mere coincidence. A similar relationship is observed for the IOD mode as well i.e. heatwaves during its positive and negative phase co-occur for an almost similar number of days and therefore, hinted that IOD most likley don't cause heatwaves in the NAS during summer months. On the other hand, as seen in the correlation maps, the negative phase of NAO likely contributes to the genesis of MHWs in the SEAS with close to 20% of heatwave days coincide with this mode during this season.

6 Dynamical mechanisms

The dynamical processes responsible for the genesis of MHWs across the global ocean vary significantly (Helbrook et al., 2019). The processes involved in the generation of heatwaves in a particular region can be assessed through the analysis of heat sources and sinks in the upper mixed layer which ultimately reflects in the variation of the SST. This approach was employed earlier for the understanding of the evolution of heatwaves during the 2011 Ningaloo Nino off Western Australia (Benthuysen et al., 2014), during 2012 warming off northeastern America (Chen et al., 2014) and in the East China Sea and

https://doi.org/10.5194/os-2021-52
Preprint. Discussion started: 11 June 2021

Ocean Science Discussions

the south Yellow Sea during the summer of 2016-2018 (Gao et al., 2020). Here, we have used a similar mixed layer heat budget formulation for the Arabian Sea (see Equation 1) to understand the dominant physical processes that are likely favouring the generation of MHWs in this region for some of the years when a large number of days experience heatwaves.

Figure 7a and 8a show that mixed layer heat budget anomaly terms along with the mean seasonal SSTs for the years when prominent heatwave days observed (see Figure 3) averaged during PRM and SWM season, respectively. Model simulated mixed layer heat budget and SST anomalies are calculated based on climatology prepared based on interannual simulation for the period 1990-2018.

For the PRM season (Figure 7a), NAS and SEAS exhibit the maximum number of heatwave days during 1998, 2002, 2003, 2010 and 2016. However, the dominant processes are somewhat different for each year. For example, during 1998, rapid warming is seen over a large part of the NAS, but it is limited towards the coast in the SEAS region in the south. However, SEAS show a slightly higher number of heatwave days than the NAS. A closer look at the heat budget anomalies suggests that while surface heat flux (Q_v) contribute strongly to the warming of the NAS region, the advection and subsurface processes contribute negatively over a large part of this region. This resulted in fewer heatwaves in the north. However, in the SEAS, strong Q_v along with persistent background warm condition resulted in a higher number of heatwave days. Similarly, for 2002 and 2003, the background warm SST plays the key role in heatwave generation in the north; however, in the south Q_v, subsurface processes and advection also contribute positively. During 2010 the highest number of heatwave observed in NAS; SEAS also sees a significant number of heatwave days, but a 10-20% fewer than the NAS (Figure 2). This large number of heatwave days in NAS is also evident in the positive tendency anomaly averaged over the entire season and primarily contributed by the strong positive Q_v anomaly and the very warm pre-condition of the SST over this region. In the SEAS, the milder positive Q_v anomaly resulted in a fewer number of heatwaves than in the NAS region. On the other hand, during 2016, while strong positive Q_v anomaly contributes to the heatwave formation in the NAS, the weaker subsurface processes and advection of warm water with the warm SST pre-conditioning resulted in heatwaves in the SEAS. A split-up of the surface flux components contributing to Q_v (Figure 7b) indicates that positive Q_v anomaly over the NAS region during 1998 and 2010 is primarily driven by a weakening of latent heat loss owing to the weaker winds and positive sensible heat flux anomaly driven by the warmer air temperature. The shortwave heat flux plays a secondary role in elevating Q_v over this region.

For the SWM season (Figure 8a, b), the heatwaves show large spatial heterogeneity. The largest number of heatwave days observed in the SEAS during 2015 driven by very warm background SST which further augmented by lower latent heat loss due to weaker winds and positive shortwave anomaly owing to the El-Niño atmospheric teleconnection. A similar pre-conditioning of SST contributed to the larger heatwaves in the year 2003 and 2010 summer as well. However, during

https://doi.org/10.5194/os-2021-52
Preprint. Discussion started: 11 June 2021

summer 2002, the positive surface heat flux driven by very strong positive shortwave flux and weaker latent and sensible heat loss contributed to the genesis of heatwaves in the SEAS.

Overall, heatwave genesis and its forcing mechanisms vary considerably from year to year and also within the Arabian Sea. Case studies concerning heatwaves of a particular region during a specific season is required to understand the complete process of its evolution and decay for the respective events.

7 Summary and discussion

In this study, we have investigated the trends and genesis of the MHWs in the Arabian Sea (north of 5°N). Particularly we studied the three main metrics of heatwaves: duration, frequency and intensity for the period of 1982-2019 and rallied primarily on the OISSTv2 SST observations. Further, we have also used an ocean model simulation based on Modular Ocean Model version 5 (MOM5) to conduct a mixed layer heat budget study for understanding the underlying forcing mechanism in the genesis of such heatwave events.

Like other regions of the world ocean, we find that the Arabian Sea also experiences a rapid increase in heatwave days. At the same time, heatwave frequency shows a marginal increase, suggesting that the heatwaves have now become prolonged and in fact, sometimes persistent for an entire season in the recent decade. However, owing to the weaker SST variability due to the proximity to the equatorial region, there is no significant increase in the heatwave intensity, a parameter often used for marking these events and thus makes this region remained unexplored in terms of MHWs in other global studies. The increasing trend of heatwave days is mainly evident post-2000 era and become conspicuous after the year 2015.

A detailed study for the pre-monsoon (or spring intermonsoon) and the summer monsoon indicates that the heatwave trend varies significantly across the seasons. During pre-monsoon, an increase in heatwave days at a rate of 15-20 days/decade is evident are primarily in the northern part of the Arabian Sea and along the coast of Arabia. However, during summer, the increasing trend at a similar rate is most evident all along the coast of India and over a large part of the southeastern Arabian Sea. Noticeably, across the last four decades, the year 2010 and 2016 show the longest heatwave days during both the seasons and in fact, was persistent for the entire pre-monsoon season at few locations across the Arabian Sea. The regions of strong heatwave trends also found to be collocated with the regions of strong SST warming trend in the recent decade. An analysis of heatwave days based on detrended SST anomaly, suggests that the enormous trend in the observed heatwave days are primarily linked to the rise in the mean SST of the Arabian Sea. The switch between the dominance of SST variability to the mean SST warming happened sometime around the year 2000. However, SST variability still contributes in a significant way for the years when climate variability dominated by major climate modes and cause a major source of SST warming in this basin. A detailed study of the association of heatwave days and these climate modes indicate that the Indian Ocean Basin

https://doi.org/10.5194/os-2021-52
Preprint. Discussion started: 11 June 2021

mode (also refers as Indian Ocean warming mode) via the decaying phase of the El-Niño influence very strongly the genesis of MHWs. In fact, during pre-monsoon, when this Indian Ocean Basin Mode is most active, co-exists in more than 70-80% of heatwave days. During the summer monsoon, its influence weakens a bit over the entire Arabian Sea but remains significantly large in the southeastern Arabian Sea. However, co-existing days reduced to merely 40% in the northern part as is also evident in the correlation maps. The next most influencing climate modes are found to be El-Niño and positive IOD. Both these modes contribute to about 40-50% of heatwave days in the northern Arabian Sea during pre-monsoon. During the summer monsoon, the impact of these climate modes are relatively less but still contribute to more than 40% of heatwave days in the southeastern Arabian Sea. But, in the north, the influence of El-niño and IOD is almost negligible during this season.

A mixed layer heat budget shows a strong heterogeneity in the forcing mechanisms of the genesis of MHWs in the Arabian Sea. As already mentioned, the background SST warming is the primary mechanism of the genesis of heatwaves in the recent decade. However, the weakening of latent heat loss due to the weakening of winds driven by climatic factors contribute significantly on a regional scale. The increased shortwave radiation likely due to the anomalous clear skies driven by El-Niño atmospheric teleconnection also contributes as a secondary forcing mechanism for such events. Note, however, that this study doesn't divulge details about their evolution, sustainability and decay as the observed heatwaves in each year or season evolve differently forced by a different combination of forcing. Case studies designed for a particular heatwave event are necessary for such understanding and therefore, to be taken separately as future studies.

This rapid increase in heatwave days in the northern and southeastern Arabian Sea is likely to cause a severe impact on the physio-biogeochemical processes of this basin. One such possible impact is the recent increase in the harmful algal bloom in the Arabian Sea. Recent studies suggest that there is a manyfold increase in the harmful phytoplankton blooms in the northern Arabian Sea and along the west coast of India attributed primarily to the increased stratification, weaker winds and warming of the Arabian Sea (Padmakumar et al., 2012; Al Shehhi et al., 2014; Goes et al., 2020). Considering that the region of increased toxic blooms are collocated with the regions where the heatwave days observed, the possibility that the relation between these heatwave events and triggering of harmful blooms can not be negated.

Another possible implication of these increase heatwave days is the increased cyclogenesis over the Arabian Sea. Dramatically, while earlier most of these tropical cyclones used to be towards the coast of Arabia (Figutre 9a), in a recent development, in the last few years severe cyclones are hitting the west coast of India. One such cyclone in the recent year was *Nisarga* which made landfall in Mumbai (a city located on the west coast of India) in summer 2020 and wracked havoc by causing loss of life and property over a vast area. Interestingly, this cyclone ended a one half month persistent heatwave of intensity more than 1^{o}C along the west coast of India (Figure 9b). It is not clear though if this intense heatwave over a vast area off the west coast of India had any influence on the genesis of this cyclone. Interestingly, while we are writing this

https://doi.org/10.5194/os-2021-52
Preprint. Discussion started: 11 June 2021

Ocean Science Discussions
Open Access
EGU

paper, another severe cyclone *Tauktae* hit the west coast of India and cause large damage to the property and life and this time as well the SST was more than 31°C off the west coast of India. Hence, there is a clear association between the heatwaves and the increased cyclogenesis along the west coast in the last few years. Further study is required to understand the dynamical link between them.

In summary, this study documented marine heatwaves and their various characteristics in the Arabian Sea. This is the first study where a detailed analysis of marine heatwave for the Arabian Sea, particularly for the coastal water of economic importance is discussed. This will give the opportunity to further investigate the impact of the heatwave events on the coastal ecosystem and other oceanic properties of this tropical basin.

Author contribution

AC designed the study and wrote the paper, AC and GA performed the data analysis, LRS conducted the model experiments and analysed the heat budget component. All authors contributed in the developing the research and contribute in discussion.

Competing interests

The authors declare no competing interests.

Data availability

The daily OISST is obtained from https://coastwatch.pfeg.noaa.gov/erddap/. The daily north Atlantic oscillation index was provided by by NCEP Climate Prediction Centre (https://ftp.cpc.ncep.noaa.gov/cwlinks/). The best track data for cyclones are obtained from "Best Track Archive" of Joint Typhoon Warning Centre. The model simulations will be made available upon request. The marine heatwave detection tool heatwaveR was taken from https://robwschlegel.github.io/heatwaveR/index.html.

Acknowledgement

The lead author thank the support provided by the Indian National Centre for Information Services (INCOIS), Ministry of Earth Sciences to carry out this research. The model simulations are carried out in the Ministry of Earth Science's central HPC facility "MIHIR". A part of this work is based on the master's dissertation thesis of GA conducted at INCOIS. LRS. was supported by the funding from INSPIRE DST fellowship. All the plotting and data analysis was carried out using R and Ferret software. This is INCOIS contribution number 0000.

https://doi.org/10.5194/os-2021-52
Preprint. Discussion started: 11 June 2021

References

Ajayamohon, R. S. and Suryachandra A. R.: Indian Ocean Dipole Modulates the Number of Extreme Rainfall Events over India in a Warming Environment, J. Met. Soc. Japan, 1, 245-252, 2008.

Al Shehhi, M. R., Gherboudj, I., Ghedira, H.: An overview of historical harmful algae blooms outbreaks in the Arabian Seas. Mar Pollut Bull., 86 (1-2), 314-324, 10.1016/j.marpolbul.2014.06.048, 2014.

Arias- Ortiz, A., Serrano, O., Masqué, P., Lavery, P. S., Mueller, U., Kendrick, G. A., Rozaimi, M., Esteban, A., Fourqurean, J. W., Marbà, N., Mateo, M. A., Murray, K., Rule, M. J., and Duarte C. M.: A marine heatwave drives massive losses from the world's largest seagrass carbon stocks. *Nat. Clim. Change* **8**, 338–344, https://doi.org/10.1038/s41558-018-0096-y, 2018.

Benthuysen, J., Feng, M. & Zhong, L.: Spatial patterns of warming off Western Australia during the 2011 Ningaloo Nino: Quantifying impacts of remote and local forcing. Cont. Shelf Res., 91, 232-246, 2014.

Benthuysen, J. A., Oliver, E. C. J., Feng, M., and Marshall, A. G. Extreme marine warming across tropical Australia during austral summer 2015–2016, J. Geophys. Res. 123, 1301–1326, 2018.

Bond, N. A., Cronin, M. F., Freeland, H., and Mantua, N.: Causes and impacts of the 2014 warm anomaly in the NE Pacific. Geophys. Res. Lett., 42**,** 3414–3420, 2015.

Caputi, N., Kangas, M., Denham, A., Feng, M., Pearce, A., Hetzel, Y., Arani, C.: Management adaptation of invertebrate fisheries to an extreme marine heatwave event at a global warming hot spot, Ecology and Evolution*,* 6(11), 3583–3593, https://doi.org/10.1002/ece3.2137, 2016.

Chatterjee, A., Shankar, D., Shenoi, S., Reddy, G., Michael, G., Ravichandran, M., Gopalkrishna, V. V., Rao, E. P. R., Bhaskar, T. V. S. U., and Sanjeevan, V. N. : A new atlas of temperature and salinity for the North Indian Ocean, Journal of Earth System Science, 121(3), 559–593, 2012.

Chatterjee, A., Shankar, D., McCreary, J., and Vinayachandran, P.: Yanai waves in the western equatorial Indian Ocean, Journal of Geophysical Research: Oceans, 118, 1556–1570, https://doi.org/0.1002/jgrc.20121, 2013.

Chatterjee, A., Shankar, D., McCreary, J., Vinayachandran, P., and Mukherjee, A.: Dynamics of Andaman Sea circulation and its role in connecting the equatorial Indian Ocean to the Bay of Bengal. Journal of Geophysical Research: Oceans, 122, 3200–3218. https://doi.org/10.1002/2016JC012300, 2017.

Chatterjee, A., Kumar, B. P., Prakash, S., and Singh, P.: Annihilation of the Somali upwelling system during summer monsoon, Scientific reports, 9(1), 7598. https://doi.org/10.1038/s41598-019-44099-1, 2019.

Chen, K., Gawarkiewicz, G. G., Lentz, S. J., Bane, J. M.:Diagnosing the warming of the northeastern U.S. coastal ocean in 2012: a linkage between the atmospheric jet stream variability and ocean response, J. Geophys. Res. Oceans, 119:218–27, 2014.

Chowdary, J. S. and Gnanaseelan, C.: Basin-wide warming of the Indian Ocean during El Niño and Indian Ocean dipole years, Int. J. of Clim., 27, 1421-1438, https://doi.org/10.1002/joc.1482, 2007, 2007.

Chakravorty, S., Chowdary, J. S., Gnanaseelan, C.: Epochal changes in the seasonal evolution of Tropical Indian Ocean warming associated with El Niño, Climate Dynamics, 42, 805-822, doi:10.1007/s00382-013-1666-3, 2014.

https://doi.org/10.5194/os-2021-52
Preprint. Discussion started: 11 June 2021

Cavole, L. M., Alyssa, M. D., Rachel, E. D., Ashlyn, G., Irina, K., Camille, M. L. S. P., May-Linn, P., Arturo, R.-V., Sarah, M. S., Nicole, K. Y., Michelle, E. Z., and Peter, J.S.:Biological Impacts of the 2013–2015 warm- water anomaly in the northeast Pacific: winners, losers, and the future, Oceanography, 29, 273–285, https://doi.org/10.5670/oceanog.2016.32, 2016.

CMFRI, 2007a. Marine fisheries profile India, http://www.cmfri.org.in/data-publications-/5/2007.

Du, Y., Xie, S.-P., Huang, G. and Hu, K.: Role of air–sea interaction in the long persistence of El Niño–induced North Indian Ocean warming. *J. Climate*, **22**, 2023–2038, 2009.

Durazo, R., and Baumgartner, T. R.: Evolution of oceanographic conditions off Baja California. Prog. Oceanogr. 54, 7–31, 2002.

Gao, G., Marin, M., Feng, M., Yin, B., Yang, D., Feng, X., Ding, Y., Song, D.: Drivers of marine heatwaves in the East China Sea and the South Yellow Sea in three consecutive summers during 2016–2018, Journal of Geophysical Research:Oceans, 125, e2020JC016518, https://doi.org/10.1029/2020JC016518, 2020.

Goes, J.I., Tian, H., Gomes, H.d.R., Anderson, O. R., Khalid, A.-H., deRada, S., Luo, H., Lubna, A.-K., Adnan, A.-A., Martinson, D. G.: Ecosystem state change in the Arabian Sea fuelled by the recent loss of snow over the Himalayan-Tibetan Plateau region. Sci. Rep., 10, 7422, https://doi.org/10.1038/s41598-020-64360-2, 2020.

Griffies, S.M., and Hallberg, R.W.: Biharmonic friction with a Smagorinsky-like viscosity for use in large-scale eddy-permitting ocean models, MonthlyWeather Review, 128(8), 2935–2946, 2000.

Griffies, S. M.: Elements of the modular ocean model (MOM), GFDL Ocean Group Tech. Rep, 7, 620, 2012.

Hobday, A. J., Alexander, L. V., Perkins, S. E., Smale, D. A., Straub, S. C., Oliver, E. C. J., Benthuysen, J. A., Burrows, M. T., Donat, M. G., Feng, M., Holbrook, N. J., Moore, P. J., Scannell, H. A., Gupta, A. S., Wernberg, T.: A hierarchical approach to defining marine heatwaves, Prog. Oceanogr., 141:227–38, 2016.

Holbrook, N. J., Scannell, H. A., Gupta, A. S., Benthuysen, J. A., Feng, M., Oliver, E. C. J., Alexander, L. V., Burrows, M. T., Donat, M. G., Hobday, A. J., Moore, P. J., Perkins-Kirkpatrick, S. E., Smale, D. A., Straub, S. C., Wernberg, T.: A global assessment of marine heatwaves and their drivers. *Nat. Commun.* 10:2624, 2019.

Holbrook, N.J., Sen Gupta, A., Oliver, E.C.J., Hobday, A. J., Benthuysen, J. A, , Scannell, H. A., Smale, D. A., and Wernberg, T.: Keeping pace with marine heatwaves, Nat. Rev. Earth Environ., 1, 482–493, https://doi.org/10.1038/s43017-020-0068-4, 2020.

Hughes, T. P., Kerry, J. T. and Wilson, S. K.: Global warming and recurrent mass bleaching of corals. Nature, 543, 373–377, https://doi.org/10.1038/nature21707, 2017.

Joseph, P. V.: Warm pool over the Indian Ocean and monsoon onset, Trop. Ocean Atmos. Newsl., Winter, 53, 1 – 5, 1990.

Kalnay, E., Kanamitsu, M., Kistler, R., Collins, W., Deaven, D., Gandin, L., Iredell, M., Saha, S., White, G., Woollen, J., Zhu, Y., Chelliah, M., Ebisuzaki, W., Higgins, W., Janowiak, J., Mo, K. C., Ropelewski, C., Wang, J., Leetmaa, A., Reynolds, R., Jenne, R., and Joseph, D.: The NCEP/NCAR 40-year reanalysis project, Bull. Am. Meteorol. Soc., 77, 437–471, 1996.

https://doi.org/10.5194/os-2021-52
Preprint. Discussion started: 11 June 2021

Klein, S. A., Soden, B. J. and Lau, N.-C.: Remote sea surface temperature variations during ENSO: Evidence for a tropical atmospheric bridge. *J. Climate*, **12**, 917–932, 1999.

Lee S.-K., Park, W., Baringer, M. O., Gordon, A. L., Huber, B., and Liu, Y.: Pacific origin of the abrupt increase in Indian Ocean heat content. Nature Geoscience, 8, 445-449, 2015.

Lakshmi, R. S., Chatterjee, A., Prakash, S., and Mathew, T.: Biophysical interactions in driving the summer monsoon chlorophyll bloom off the Somalia coast. Journal of Geophysical Research: Oceans, 125, https://doi.org/10.1029/2019JC015549, 2020.

Large, W. G., McWilliams, J. C., and Doney, S. C.: Oceanic vertical mixing: A review and a model with a nonlocal boundary layer parameterization. Reviews of Geophysics, 32(4), 363–403, 1994.

Levitus, S., Antonov, J. I., Boyer, T. P., Baranova, O. K., Garcia, H. E., Locarnini, R. A., Mishonov, A. V., Reagan, J. R., Seidov, D., Yarosh, E. S. and Zweng, M. M.: World ocean heat content and thermosteric sea level change (0–2000 m), 1955–2010. Geophysical Research Letters 39(10). doi:10.1029/2012GL051106, 2012.

Lorenzo, E. D., Mantua, N.: Multi-year persistence of the 2014/15 North Pacific marine heatwave, Nature Cli. Change, 6, https://www.nature.com/articles/nclimate3082, 2016.

Mills, K. E., Andrew, J. P., Curtis, J. B., Yong, C., Fu-Sung, C., Daniel, S. H., Sigrid, L., Janet, A. N., Jenny, C. S., Andrew, C. T., Richard, A. W.:Fisheries management in a changing climate: lessons from the 2012 ocean heat wave in the Northwest Atlantic. *Oceanography* **26**, 191–195, 2013.

Holbrook, N. J., Scannell, H. A., Gupta, A. S., Benthuysen, J. A., Feng, M., Oliver, E. C. J., Alexander, L. V., Burrows, M. T., Donat, M. G., Hobday, A. J., Moore, P. J., Perkins-Kirkpatrick, S. E., Smale, D. A., Straub, S. C., Wernberg, T.: A global assessment of marine heatwaves and their drivers. *Nat. Commun.* 10:2624, 2019.

Olita, A., Sorgente, R., Ribotti, A., Natale, S., and Gaberšek, S.: Effects of the 2003 European heatwave on the Central Mediterranean Sea surface layer: a numerical simulation. Ocean Sci. Discuss, 3, 85–125 (2006).

Oliver, E. C. J., Benthuysen, J. A., Bindoff, N. L., Hobday, A. J., Holbrook, N. J., Mundy, C. N., Perkins-Kirkpatrick, S. E.: The unprecedented 2015/16 Tasman Sea marine heatwave. *Nat. Commun.* 8:16101, 2017.

Oliver, E.C., Burrows, M.T., Donat, M.G., Sen Gupta, A., Alexander, L.V., Perkins-Kirkpatrick, S.E., Benthuysen, J., Hobday, A.J., Holbrook, N.J., Moore, P. J., and Thomsen, M. S.: Projected marine heatwaves in the 21st century and the potential for ecological impact, Front. Mar. Sci., 6, p.734, 2019.

Oliver, E. C. J., Benthuysen, J. A., Darmaraki, S., Donat, M. G., Hobday, A. J., Holbrook, N. J., Schlegel, R. W., Gupta, A. S.: Marine heatwaves, Ann. Rev. Mar. Sci., 13, 313-342, https://doi.org/10.1146/annurev-marine-032720-095144 , 2021.

Padmakumar, K. B., Menon, N. R., Sanjeevan, V. N.: Is Occurrence of Harmful Algal Blooms in the Exclusive Economic Zone of India on the Rise? Int. J. of Ocean., 2012, 1-7, https://doi.org/10.1155/2012/263946, 2012.

Papa, F., Durand, F., Rossow, W. B., Rahman, A., and Bala, S. K.: Satellite altimeter-derived monthly discharge of the Ganga-Brahmaputra River and its seasonal to interannual variations from 1993 to 2008, Journal of Geophysical Research, 115, C12013, https://doi.org/10.1029/2009JC006075, 2010.

Pearce, A. F., Lenanton, R., Jackson, G., Moore, J., Feng, M., Gaughan, D.: The "marine heat wave" off Western Australia during the summer of 2010/11, Tech. Rep. 222, West. Aust. Fish. Mar. Res. Lab., North Beach, Australia, 2011.

Praveen, K. B., Vialard, J., Lengaigne, M., Murty, V., and Mcphaden, M. J.: TropFlux: Air-sea fluxes for the global tropical oceans-description and evaluation. Climate Dynamics, 38(7-8), 1521–1543, 2012.

Praveen, K. B., Vialard, J., Lengaigne, M., Murty, V., Mcphaden, M. J., Cronin, M., Pinsard, F., Gopala, R. K.: TropFlux wind stresses over the tropical oceans: Evaluation and comparison with other products. Climate Dynamics, 40(7-8), 2049–2071, 2013.

Reynolds, R. W., Smith, T. M., Liu, C., Chelton, D. B., Casey, K. S., and Schlax, M. G.: Daily high-resolution-blended analyses for sea surface temperature, Journal of Climate, 20(22), 5473–5496, https://doi.org/10.1175/2007JCLI1824.1, 2007.

Roxy, M., Ritika, K., Terray, P. and Masson, S.: The curious case of Indian Ocean warming, *J. Climate*, 27, 22, 8501-8509, 2014.

Roxy, M., Ritika, K., Terray, P., Murtugudde, R., Ashok, K., Goswami, B. N.: Drying of Indian subcontinent by rapid Indian Ocean warming and a weakening land-sea thermal gradient. Nat. Commun., 6, https://doi.org/10.1038/ncomms8423, 2015.

Roxy, M. K., Modi, A., Murtugudde, R., Valsala, V., Panickal, S., Prasanna, K. S., Ravichandran, M., Vichi, M., and Lévy M.: A reduction in marine primary productivity driven by rapid warming over the tropical Indian Ocean, Geophys. Res. Lett., 43, 826–833, doi:10.1002/2015GL066979, 2016.

Roxy, M. K. , Gnanaseelan, C., Parekh, A., Chowdary, J. S., Singh, S., Modi, A., Kakatkar, R., Mohapatra, S., and Dhara, C.: Indian Ocean warming, In Assessment of Climate Change over the Indian Region, Krishnan, R., Sanjay, J., Gnanaseelan, C., Mujumdar, M., Kulkarni, A., Chakraborty, S., Eds., Springer, https://doi.org/10.1007/978-981-15-4327-2, 2020.

Saji, N. H., Goswami, B. N. , Vinayachandran, P. N. and Yamagata, T.: A dipole mode in the tropical Indian Ocean. *Nature*, **401**, 360–363. 1999.

Salinger MJ, Renwick J, Behrens E, Mullan AB, Diamond HJ, Sirguey, P., Smith, R. O., Trought, M. C. T., Alexander V, L., Cullen, N. J.: The unprecedented coupled ocean-atmosphere summer heatwave in the New Zealand region 2017/18: drivers, mechanisms and impacts. Environ. Res. Lett., 14:044023, 2019.

Scannell, H. A., Pershing, A. J., Alexander, M. A., Thomas, A. C. and Mills, K. E.: Frequency of marine heatwaves in the North Atlantic and North Pacific since 1950, Geophys. Res. Lett., 43, 2015GL067308, 2016.

Schlegel, R. W. and Smit, A. J.: heatwaveR: A central algorithm for the detection of heatwaves and cold-spells. Journal of Open Source Software, 3(27), 821, https://doi.org/10.21105/joss.00821, 2018.

Shankar, D., Remya, R., Vinayachandran, P., Chatterjee, A., and Behera, A.: Inhibition of mixed-layer deepening during winter in the northeastern Arabian Sea by theWest India Coastal Current, Climate Dynamics, 47(3-4), 1049–1072, 2016.

https://doi.org/10.5194/os-2021-52
Preprint. Discussion started: 11 June 2021

Ocean Science Discussions Open Access EGU

Shankar, D., Remya, R., Anil, A. C., and Vijith, V.: Role of physical processes in determining the nature of fisheries in the eastern Arabian Sea, 172 (12), 10.1016/j.pocean.2018.11.006, 2018.

Shenoi, S. S. C., Shankar, D. and Shetye, S. R.: On the sea surface temperature high in the Lakshadweep Sea before the onset of southwest monsoon, J. Geophys. Res., 104(C7), 15703 – 15712, 1999.

Sindhu, B., Suresh, I., Unnikrishnan, A., Bhatkar, N., Neetu, S., and Michael, G.: Improved bathymetric datasets for the shallow water regions in the Indian Ocean, Journal of Earth System Science, 116(3), 261–274, 2007.

Swapna, P., Krishnan, R. and Wallace, J.M.: Indian Ocean and monsoon coupled interactions in a warming environment. Clim Dyn, 42**,** 2439–2454, https://doi.org/10.1007/s00382-013-1787-8, 2014.

Trainer, V. L., Kudela, R. M., Hunter, M. V., Adams, N. G., and McCabe, R. M.: Climate Extreme Seeds a New Domoic Acid Hotspot on the US West Coast, Front. Clim., 2:571836, doi: 10.3389/fclim.2020.571836, 2020.

Thomsen, M. S., Mondardini, L., Alestra, T., Gerrity, S., Tait, L., South, P. M., Lilley, S. A., Schiel, D. R.: Local extinction of bull kelp (*Durvillaea* spp.) due to a marine heatwave, Front. Mar. Sci. 6, 84, https://doi.org/10.3389/fmars.2019.00084, 2019.

Vijith, V., Vinayachandran, P., Thushara, V., Amol, P., Shankar, D., and Anil, A.: Consequences of inhibition of mixed-layer deepening by the West India Coastal Current for winter phytoplankton bloom in the northeastern Arabian Sea, Journal of Geophysical Research: Oceans, 121, 6583–6603, https://doi.org/10.1002/2016JC012004, 2016.

Vinayachandran, P. N., and Shetye, S. R.: The warm pool in the Indian Ocean, Proc. Indian Acad. Sci. (Earth Planet. Sci.), 100(2), 165 – 175., 1991.

Vörösmarty, C., Fekete, B., and Tucker, B.: River discharge database, Version 1.0 (RivDIS v1. 0), Volumes 0 through 6. A contribution to IHP-V Theme: 1. Technical documents in hydrology series. Paris: UNESCO, 1996.

Wernberg, T., Bennett, S., Babcock, R. C., De Bettignies, T., Cure, K., et al.: Climate- driven regime shift of a temperate marine ecosystem, Science, 353, 169–172, 2016.

Xie, S. P., Hu, K., Hafner, J., Tokinaga, H., Du, Y., Huang, G., and Sampe, T.: Indian Ocean capacitor effect on Indo-Western Pacific climate during the summer following El Nino. J. Clim. 22, 730-747 (2009).

Xie, T., Li, J., Chen, Chen, K., Zhang, Y., Sun, C.: Origin of Indian Ocean multidecadal climate variability: role of the North Atlantic Oscillation. Clim Dyn, 56**,** 3277–3294, https://doi.org/10.1007/s00382-021-05643-w, 2021.

https://doi.org/10.5194/os-2021-52
Preprint. Discussion started: 11 June 2021

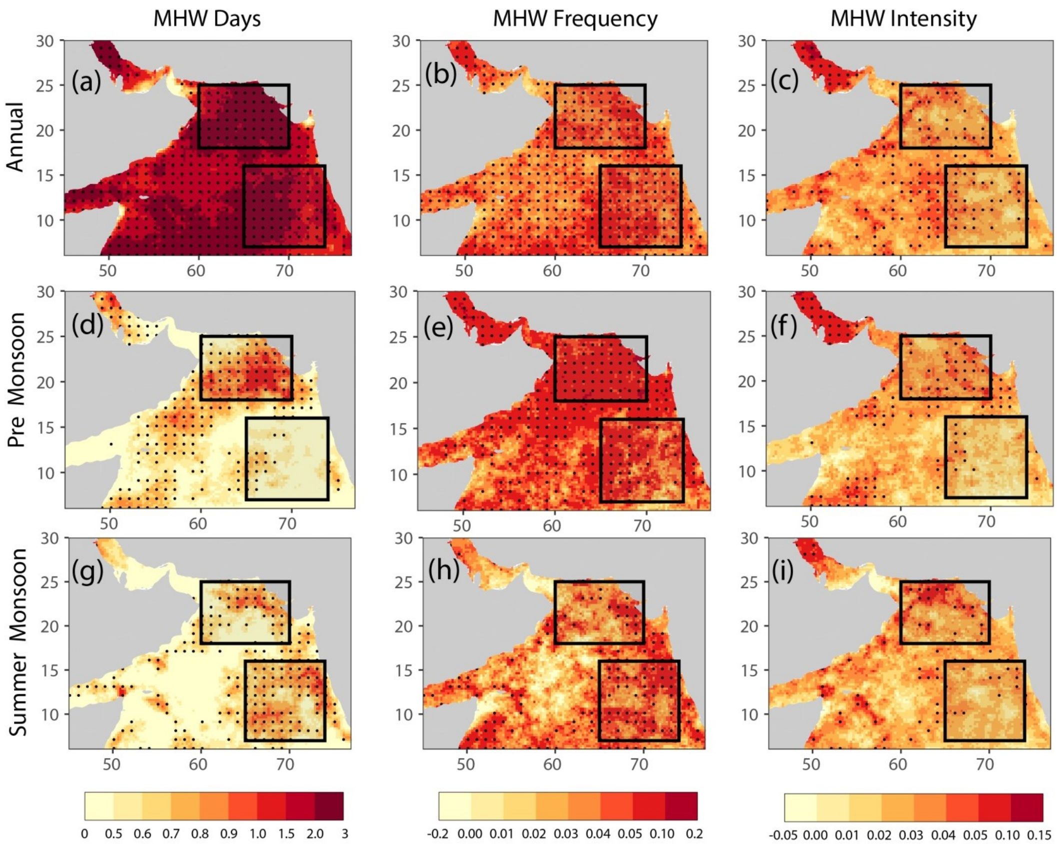

Figure 1: Trend for the MHW days (days/year; left panels), MHW frequency (count/year; middle panels) and MHW intensity (°C/year; right panels) for the annual (a,b,c), pre-monsoon (d,e,f) and summer monsoon (g,h,i) periods. The trends within the 99% confidence limit are marked by stapling. The black boxes represent the north Arabian Sea (NAS) and the southeastern Arabian Sea (SEAS).

https://doi.org/10.5194/os-2021-52
Preprint. Discussion started: 11 June 2021

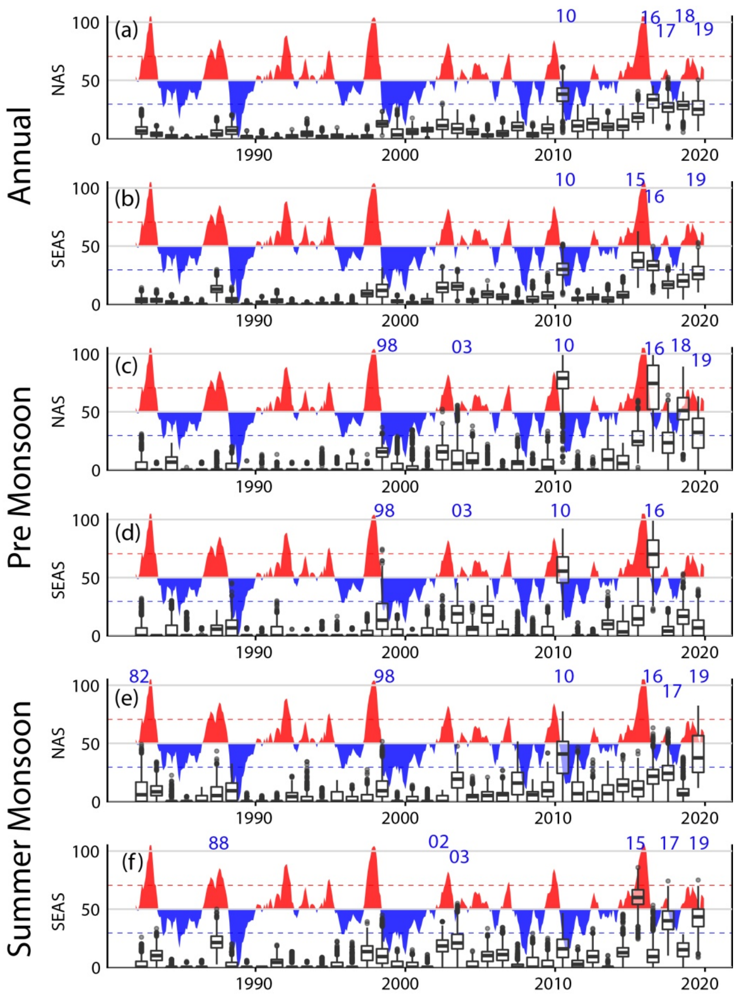

Figure 2: Boxplots of heatwave days using OISST during (a,b) annual, (c,d) pre-monsoon and (e,f) summer monsoon season for the north Arabian Sea (NAS) and the southeastern Arabian Sea (SEAS). The shading represents Niño3.4 index and red and blue dashed lines represent its 0.5 standard deviations. The numbers in blue fonts on top of each panels highlight the years when number of heatwave days are comparatively larger than the other years.

https://doi.org/10.5194/os-2021-52
Preprint. Discussion started: 11 June 2021

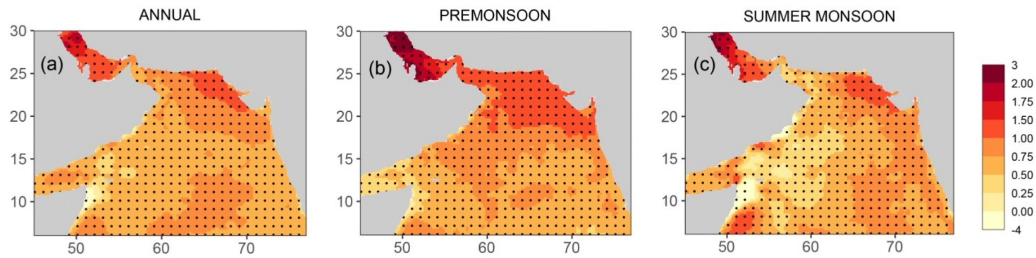

Figure 3: Trends of SST (°C/37 years) over 1982-2019 for (a) annual, (b) pre-monsoon and (c) summer monsoon period. Stiplings show regions where the trend is 99% significant based on two-tailed t-test.

https://doi.org/10.5194/os-2021-52
Preprint. Discussion started: 11 June 2021

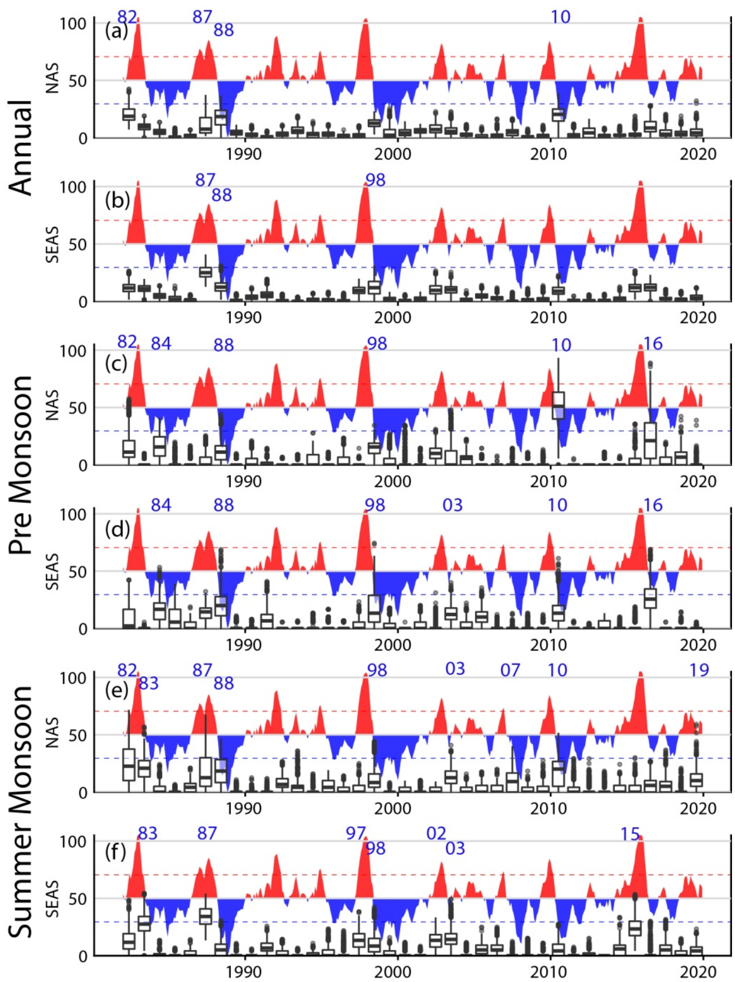

Figure 4: same as Figure 2, but using the detrended SST (T^{var}).

https://doi.org/10.5194/os-2021-52
Preprint. Discussion started: 11 June 2021

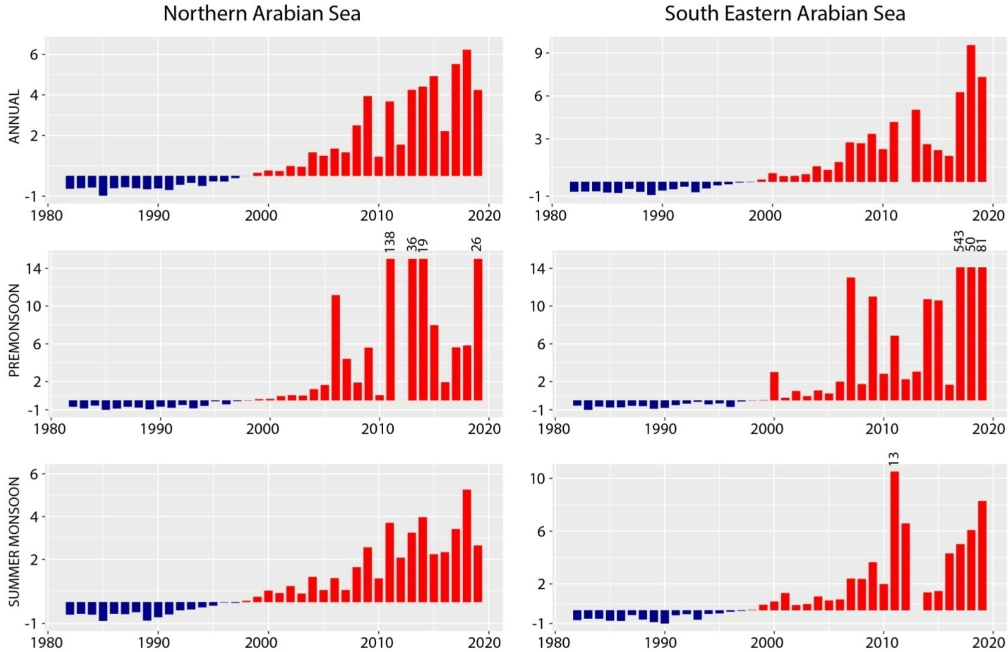

592

593 **Figure 5:** Ratio of MHW days derived using SST (T) and detrended SST (T^{var}) based on Equation (3).

594

https://doi.org/10.5194/os-2021-52
Preprint. Discussion started: 11 June 2021

Ocean Science
Discussions

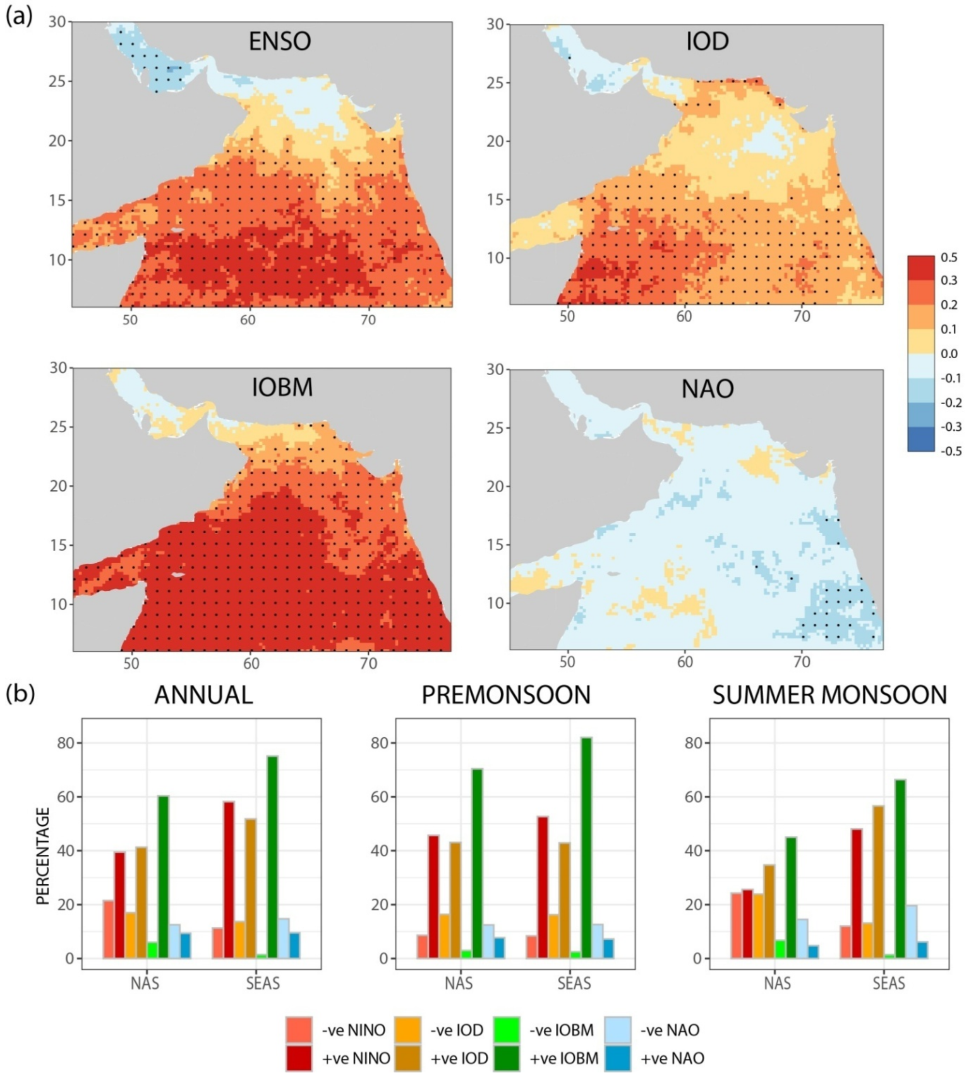

595

596 **Figure 6:** (a) Correlation between MHW days based on detrended SST (T^{var}) and major climate modes. Staplings represents regions
597 where correlations are 99% significant. (b) Percentage of co-existing days between observed heatwaves and climate modes for annual, pre-
598 monsoon and summer monsoon period.

599

https://doi.org/10.5194/os-2021-52
Preprint. Discussion started: 11 June 2021

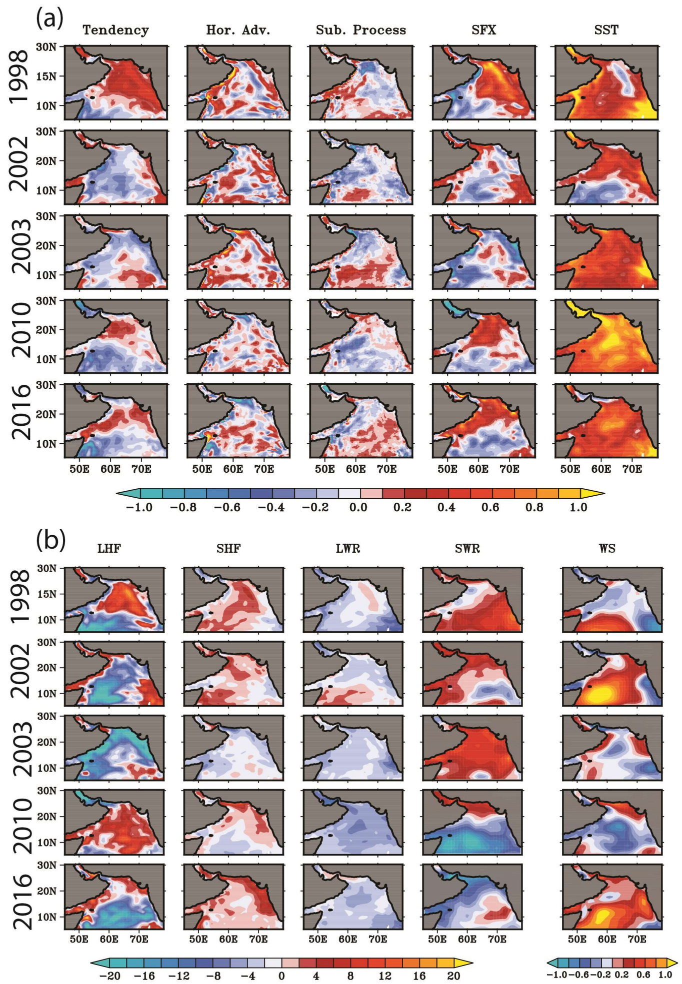

Figure 7: (a) seasonally averaged (pre-monsoon; MAM) anomalies of the temperature tendency (°C/month) and role of horizontal avection, subsurface processes and the net surface heat flux (Q_v) on the simulated tendency. (right column) SST anomalies during the pre-monsoon season. (b) Seasonally averaged (pre-monsoon) surface heat flux components i.e latent heat flux (LHF), sensible heat flux (SHF), Net logwave radiation (LWR) and surface shortwave radiation (SWR). (right column) wind speed anomaly during the pre-monsoon season.

https://doi.org/10.5194/os-2021-52
Preprint. Discussion started: 11 June 2021

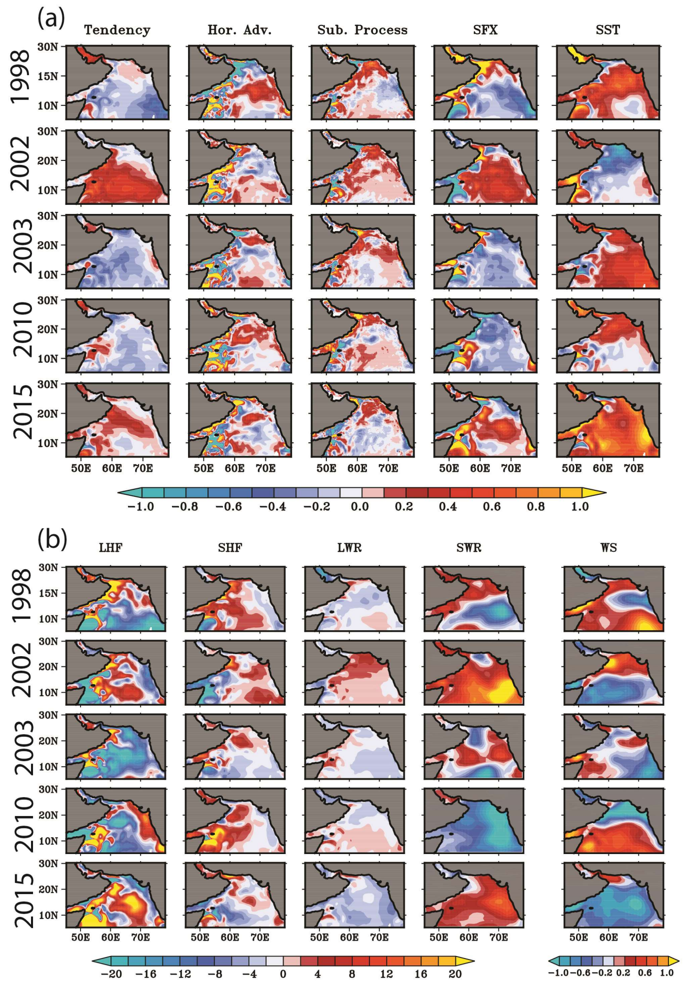

Figure 8: Same as Figure 7, but for the summer monsoon (JJAS) season.

https://doi.org/10.5194/os-2021-52
Preprint. Discussion started: 11 June 2021

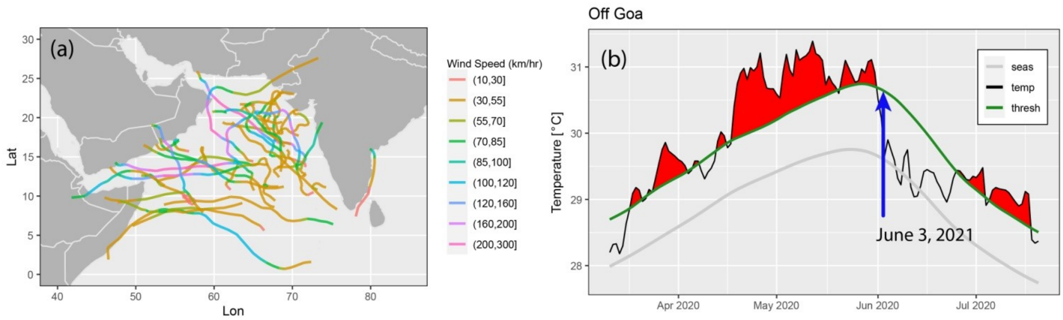

Figure 9: (a) All cyclone best tracks in the Arabian Sea during 2000-2019. The intensity of the wind speed are deonted by the color scale. All cyclones usually originate in the southern Arabian Sea and move towards the coast of Arabia. (b) SST (temp, black line) just before the cyclone Nisarga which had a longfall at Mumbai on June 3, 2020. The green line represent the 90% seasonally varying threshold, gray line is the climatology. The red shaded region shows the heatwave event.